Multiphase Coexistence in an Ionic Liquid: Violation of Gibbs Phase Rule?

Various phases appeared in a single-component 1-decyl-3-methylimidazolium nitrate ([C_{10}mim][NO_3]) ionic liquid. Time-resolved synchrotron small- and wide-angle X-ray scattering (SWAXS) could distinguish the phase transitions depending upon the cooling rate. On the SWAXS patterns, low-*Q* peaks representing a few kinds of layered structures were decomposed. Multiphase coexistence was observed in [C_{10}mim][NO_3] at the specific cooling rates (8–9 K/min). Ionic liquid crystal, hybrid-layered crystal, and hexagonal close-packed structure coexisted simultaneously. Multiphase coexistence was induced in the vicinity of a multiphase coexistence point.

A Gibbs phase rule describes the degree of freedom of a multiphase system under equilibrium conditions. A quadruple point was found even in a single-component system using the Monte Carlo simulations [1]. Recently, a generalized Gibbs phase rule was proposed with additional parameters [1, 2].

Ionic liquids (ILs) consisting of a cation and an anion are characterized by nanoheterogeneous liquid structures [3]. The representative cation is 1-alkyl-3-methylimidazolium, [$C_n$mim]$^+$, where *n* reveals the alky chain length. Various phases in [$C_n$mim][X] appeared on the *n*-temperature (*T*) plot (Fig. 1) [4]. A multiphase coexistence point (MCP) locates in the vicinity of *n* = 10. Conformational polymorph of [$C_n$mim][NO_3] (*n* = 4, 6, and 8) was examined at high pressure (HP), relating to HP multiple-glass transitions [5]. The stable conformers of [C_{10}mim]$^+$ were evaluated using density fluctuation theory (DFT) (Fig. 2) [6]. The conformers of [C_{10}mim]$^+$ in the crystal states were observed using Raman spectroscopy. Moreover, crystal structures of [C_{10}mim][NO_3] were determined at low temperature (LT) and HP using

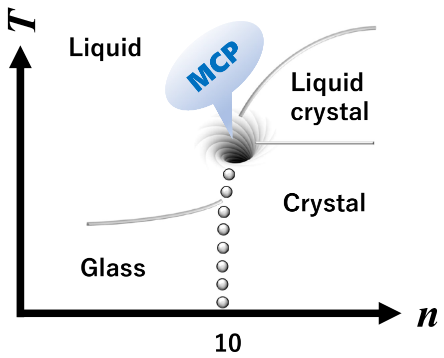

Figure 1: Phase diagram of [$C_n$mim][X] on the *n* and temperature (*T*) scales.

synchrotron small- and wide-angle X-ray scattering (SWAXS) [7]. A hybrid-layered structure with a lattice constant of 4.3 nm appeared at both LT and HP. [C_{10}mim][NO_3] was found to be flexible by pressure dependence of the lattice constants [7]. Here, we emphasize that the LT crystal polymorph was different from that at HP due to the packing polymorph. Cooling-rate dependent phase behaviors of [C_{10}mim][NO_3] were clarified using simultaneous SWAXS and differential scanning calorimetry (DSC) measurements [8]. Drastic phase changes were induced at a cooling rate of 8.1 K/min. Three broad exothermal peaks appeared on the DSC thermal trace at 8.1 K/min. Since the cooling rate was high, the phase changes were not distinguished using an *in-house* X-ray generator.

An *in-situ* observation is indispensable to extract hidden information about the complicated phase behaviors of [C_{10}mim][NO_3]. Synchrotron SWAXS with a high performance 2D detector (*PILATUS*) can obtain time-resolved 2D patterns even at the cooling rate of 20 K/min. For instance, the 2D SWAXS pattern of [C_{10}mim][NO_3] at 8 K/min is shown in Fig. 3. In the enlarged picture, the four Debye rings at low *Q* were observed distinctly. Generally, considering only one phase, a large unit cell is required to explain the four Bragg reflections at low *Q*. By changing the cooling rates systematically, the entirely different SWAXS patterns were detected at the minimum temperature, T_{min} (150 K) (Figs. 4(a)-4(f)). At 2 K/min, the hybrid-layered crystal (C) phase appeared in the previous study (Fig. 4(a)) [7]. At 5 K/min, the ionic liquid crystal (ILC) phase existed partially in addition to the hybrid-

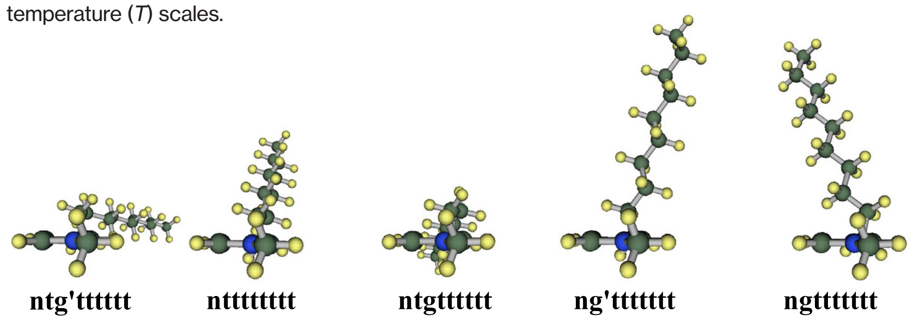

Figure 2: Optimized molecular conformations of [C_{10}mim]$^+$ using DFT.

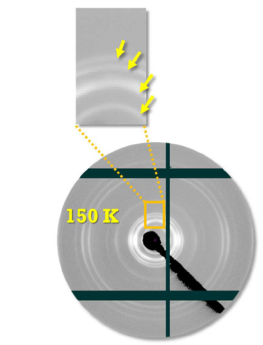

Figure 3: 2D SWAXS pattern of [C_{10}mim][NO_3] at cooling rate of 8 K/min.

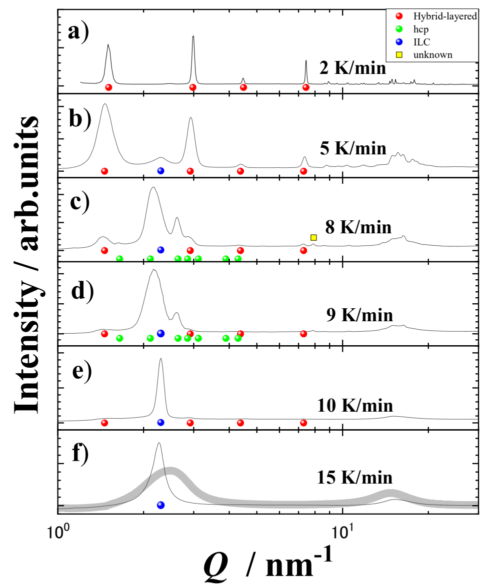

Figure 4: SWAXS patterns at 150 K with cooling rates of **(a)** 2, **(b)** 5, **(c)** 8, **(d)** 9, **(e)** 10, and **(f)** 15 K/min.

layered C phase (Fig. 4(b)). On the other hand, at 15 K/min (Fig. 4(f)), the ILC phase was preferred and the peak position was the same as the additional peak position at 5 K/min. More importantly, on the phase change from the hybrid-layered C at 2 K/min to the ILC at 15 K/min, a hexagonal close-packed (hcp) structure was induced at 8 and 9 K/min (Figs. 4(c) and 4(d)). Moreover, the amorphous halo appeared at 15 nm^{-1}. The sizes of the ILC, hybrid-layered C, and hcp phases are illustrated in Fig. 5. Since the temperature region of the ILC phase became narrower with increasing cooling rate [6, 8] (Fig. 1), the cooling path at 8 K/min could be approaching to the MCP. Here, we deduce that the specific fluctuations in the vicinity of the MCP caused the hcp phase at 8 K/min. The multiphase coexistence at 8 K/min is derived from the following three factors; (i) a flexible alkyl chain of [C_{10}mim]$^+$, (ii) conformational polymorph of [C_{10}mim]$^+$, and (iii) the specific fluctuations in the vicinity of the MCP. Based on three factors, we assume that alkyl chain entanglement of [C_{10}mim]$^+$ could be influenced extensively by the cooling rates. The appearance of well-ordered ILC or distorted ILC (d-ILC) phases implies that the chain entanglement/antiparallel packing contributed to the crystalline quality. In fact, the well-ordered ILC appeared only at 8 and 9 K/min as seen in Fig. 6. Hence, in the vicinity of the MCP, the chain entanglement was suppressed at 8 and 9 K/min, and the hcp phase was formed additionally. Another significant point is that the reentrant phase transition of ILC was observed only at 8 and 9 K/min.

Time-resolved synchrotron SWAXS experiments can distinguish the cooling-rate effects for the complicated phase transitions of [C_{10}mim][NO_3]. Phase anomalies at 8 and 9 K/min in the vicinity of the MCP are summarized as follows; (i) multiphase coexistence

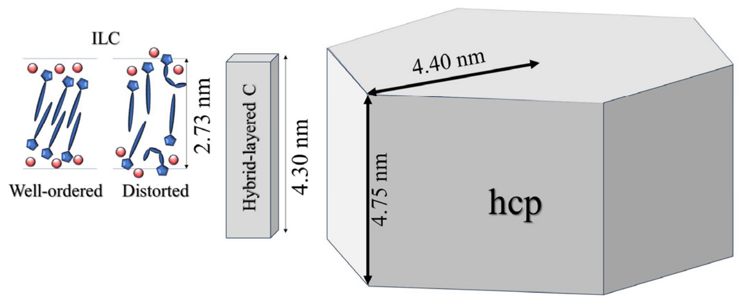

Figure 5: Sizes of the [C10mim]+ cation, well-ordered ILC, distorted ILC, hybrid-layered C, and hcp structures.

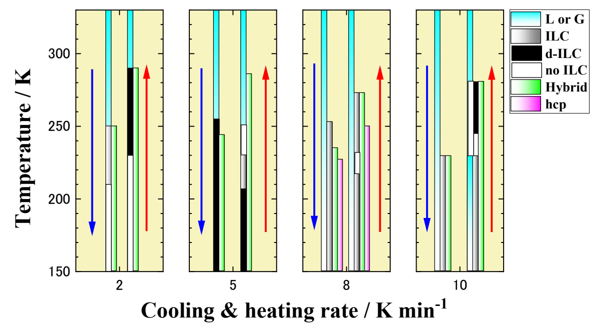

Figure 6: Cooling/heating rate dependence of the phase changes in [C_{10}mim][NO_3].

(additional hcp phase), (ii) the well-ordered ILC, and (iii) the reentrant phase transition of ILC. The well-ordered ILC, hybrid-layered C, and hcp phases coexisted with amorphous at T_{min}. If amorphous is a liquid phase near the MCP, the four phases coexistence in a single-component system could be realized (Fig. 6) At the fixed pressure, the Gibbs phase rule is provided by *F*=*C*–*N*+1, where *F*, *C*, and *N* reveal the number of degrees of freedom, the number of different components, and the number of coexisting phases, respectively [2]. Violation of the Gibbs phase rule occurred in the single-component [C_{10}mim][NO_3]?

REFERENCES

[1] K. Akahane, J. Russo and H. Tanaka, *Nature Commun.* **7**, 12599 (2016).
[2] V. F. D. Peters, M. Vis, Á. González García, H. H. Wensink and R. Tuinier, *Phys. Rev. Lett.* **125**, 127803 (2020).
[3] J. N. A. Canongia Lopes and A. A. H. Pádua, *J. Phys. Chem. B* **110**, 3330 (2006).
[4] J. D. Holbrey and K. R. Seddon, *Clean Prod. Proc.* **1**, 223 (1999).
[5] H. Abe, T. Hirano, H. Kishimura, T. Takekiyo and Y. Yoshimura, *J. Mol. Liq.* **402**, 124764 (2024).
[6] H. Abe, S. Maruyama, H. Kishimura, M. Uruichi, D. Okuyama and H. Sagayama, *J. Phys. Chem. Lett.* **15**, 10668 (2024).
[7] H. Abe, Y. Yoshiichi, H. Kishimura and H. Sagayama, *Chem. Phys. Lett.* **827**, 140685 (2023).
[8] H. Abe and H. Kishimura, *J. Mol. Liq.* **352**, 118695 (2022).

BEAMLINE

BL-8B

H. Abe[1], D. Okuyama[2] and H. Sagayama[2] ([1]National Defense Academy, [2]KEK-IMSS)